Applying the technique of ultrafast pump-probe spectroscopy on the main plant light-harvesting complex of spinach leaves

Asmita Singh, and Tjaart P J Krüger

Department of Physics, University of Pretoria, Pretoria, South Africa, 0002

E-mail: Tjaart.Kruger@up.ac.za

Abstract. The ultrafast transient dynamics of the main plant light-harvesting complex, LHCII, of spinach leaves were studied using transient absorption (TA) pump-probe spectroscopy. Explicitly, the excitation energy transfer (ET) processes within and amongst the protein-bound pigments (viz. chlorophylls (Chls) and carotenoids (Cars)) were investigated. These pigments are responsible for the absorption of solar photons and transfer the electronic excitation energy on ultrafast timescales to nearby complexes and eventually to a reaction center where charge separation is induced. We investigated differences in the ET kinetics that arise from exciting particular Cars preferentially. In particular, Lutein 1 and Neoxanthin were targeted using an excitation wavelength (λ_{ex}) of 489 nm, while Lutein 2 and Violaxanthin were excited specifically at 506 nm. Global analysis of the TA results was performed. The wavelength-dependent excitation study showed the ET dynamics to either be blue-shifted (λ_{ex} of 489 nm) or red-shifted (λ_{ex} of 506 nm) by ~5 nm. The general spectral (at the pigment peaks) and kinetic (species lifetimes) results were obtained. On average, the fluence was measured to be ~10^{17} photons per cm^2 per pulse. A high excitation fluence induces the probability of singlet-singlet annihilation to occur, thus a surplus of molecules will relax back to the ground state. This work exhibits the successful application of the ultrafast pump-probe spectroscopic technique onto the LHCII of spinach leaves, preparing a local South African system to contend with international standards.

1. Introduction

Natural photosynthesis is a vital source for food production in nature and is the chief solar energy storing process known to exist on earth. Understanding the molecular mechanisms that underlie this process is necessary for sustainable future development, especially for solar energy production as an alternative to fossil fuel energy sources.

The photosynthetic light-harvesting (LH) apparatus of a plant is comprised of intricate networks of membrane-bound pigment-protein complexes. The photosystem-II (PSII) supercomplex houses the LHCII. LHCII, which naturally assumes a trimeric arrangement of three identical subunits, contains two main types of protein-bound pigments, viz. Chls and Cars [1]. These pigments capture the solar photons and transfer the electronic excitation energy on ultrafast timescales to neighbouring complexes and eventually to a reaction center (RC), where a charge separation is initiated [2, 3]. Plants are naturally able to protect themselves against the adverse effects of over-illumination through the process of non-photochemical quenching (NPQ). During NPQ excess energy is dissipated as heat via competing ET channels amongst the pigments [4]. Cars quench Chl triplet states in order to prevent the formation of reactive singlet oxygen, which is toxic to biological entities [5]. Understanding NPQ is a stepping-stone towards improving bio-inspired solar cell devices, particularly the role of Cars in quenching the Chl excited singlet states [6].

The light absorption region of Cars in higher plants is typically 400 nm – 500 nm, followed by excited ET to Chls *a* and *b*, thus increasing the spectral cross section for photosynthetic activity [7]. The individual ET dynamics can be studied through ultrafast spectroscopic techniques, such as transient absorption (TA) pump-probe (PP) spectroscopy. Pump pulses prompt the photoinduced processes, and the ET is typically probed with a white light continuum.

In the Car electronic structure, the excited-state manifold consists of two low-lying excited singlet states, viz. S_1 and S_2. Transitions from the ground state (GS), S_0, to S_1 are a one-photon symmetry forbidden transition due to S_0 and S_1 having the same electronic inversion symmetry. In contrast, the transition from S_0 to S_2 is strongly allowed and therefore typically observed in spectroscopic signals. Upon excitation, the S_2 state rapidly decays within a few hundred femtoseconds to the optically dark (i.e. nonradiative) S_1 state, which subsequently decays on a picosecond timescale to S_0 [7]. Due to the short lifetime of S_2 its excited state absorption (ESA) is not significant [8]. The decay of the strong negative ground state bleach (GSB), which is associated with the pump λ_{ex}, enables the estimation of the S_2 lifetime [9]. Therefore, it is necessary to exploit the structure and amplitude of the ESA of S_2. In this study, we examined the TA signals of LHCII at two different λ_{ex}, exciting specific Cars, viz. 489 nm for Lutein 1 and Neoxanthin, and 506 nm for Lutein 2 and Violaxanthin.
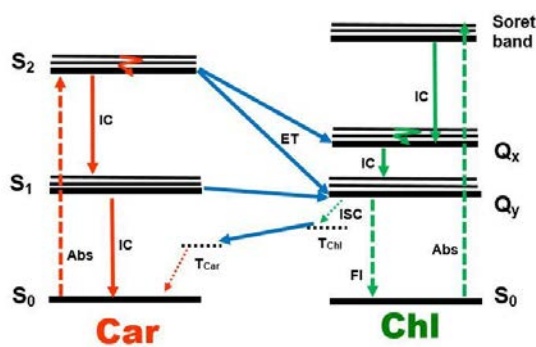

Figure 1: Simplified energy level diagram of the ET pathways between electronic excited states of Car and Chl pigment molecules, as well as the deactivation pathways within the molecules. Dotted lines show triplet states, whilst the solid lines denote singlet states. The Fl dashed arrow denotes a radiative process, solid blue is used for ET, and solid orange and green for non-radiative processes. Abs: absorption, Fl: fluorescence, IC: internal conversion, ISC: intersystem crossing.

2. Experimental

2.1. *Sample preparation*

Isolated LHCII trimers were prepared from PSII-enriched thylakoid membranes of spinach leaves [10, 11]. A buffer-detergent mixture (1.5 ml) consisting of 1.455 ml of 20 mM Hepes at pH 7.5 was added to 45 μl of 1 % weight/volume β-DM detergent.

An Agilent Technologies Cary UV-Visible spectrophotometer was used to measure the LHCII sample's absorption spectrum, identifying pigment peak absorptions. Specifically, the exact sample concentration at the Q_y^2 peak of Chl *a* was found to be at an optimal optical density (OD = εlC) of 0.725/mm, using the Beer-Lambert law

$$I = I_0 e^{-\varepsilon dC} \tag{1}$$

where *I* is the pump beam intensity after, and I_0 the intensity before the sample, ε the molar extinction coefficient [in $dm^3.mol^{-1}.cm^{-1}$], *d* the path length and *C* the concentration of the sample [in $mol.dm^{-3}$].

---

[2] Q_y transition: the longest-wavelength transition, invariably polarized along the *y*-axis of the molecule [12]

2.2. *Experimental technique*

The excited-state dynamics of isolated LHCII trimers was investigated by using the femtosecond TA PP spectroscopy laser facility of the National Laser Centre (NLC) at the Centre for Scientific and Industrial Research (CSIR) in Pretoria, South Africa.

The setup consists of a regenerative, 1 kHz amplified Ti:Sapphire solid-state laser (Clark – MXR, Inc. CPA 2110*i*). An optimal power of 1 W, with a pulse duration of 150 fs (corresponding to a transform-limited bandwidth of 7 nm) and central output peak wavelength of 775 nm was used. The CPA laser beam is split into two – one for the pump beam (30%) and one for the probe beam (70%). A non-collinear optical parametric amplifier (NOPA), pumped by the second harmonic (387.5 nm), is used to generate a pump pulse. Either a long-pass or short-pass filter at 500 nm was used outside the NOPA to narrow the spectral bandwidth for selective wavelength excitation. After prism compression, the pulse duration is ~30-40 fs, with a spectral FWHM bandwidth of 15 nm. A combination of neutral density filters were used to further tailor the pulse.

A 1 kHz mechanical chopper is used to distinguish between an excited state (pump-on) and an unexcited state (pump-off) for the pump pulse. This gives the difference in absorption (ΔA) of the sample. ΔA is probed with a broadband white-light beam, generated by a sapphire crystal. The probe pulse is delayed with respect to the pump pulse by using a 2 ns optical delay line. The pump and probe pulses overlap both spatially and temporally in the 1 mm path length cuvette that contains the prepared LHCII sample. The polarization of the pump pulse was set at the magic angle (54.7º) with respect to the probe pulse. Measurements were conducted at room temperature in aerobic conditions. To prevent photobleaching, small orthogonal vibrations were induced to the sample through the cuvette by using an amplifier.
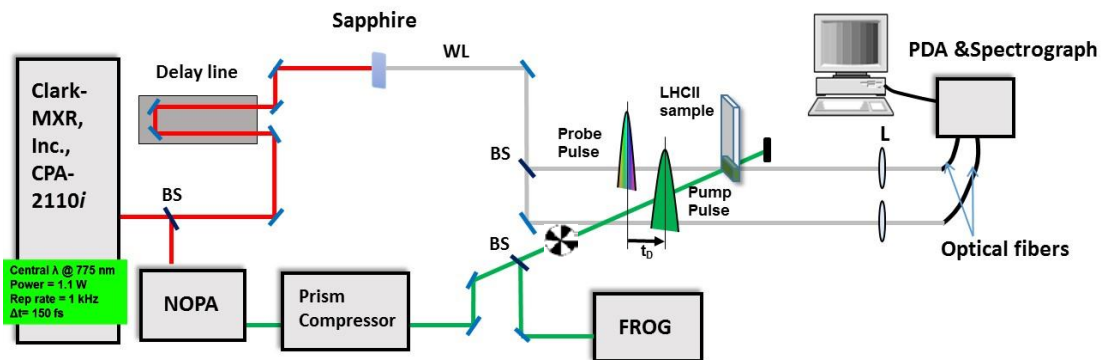

Figure 2: The TA PP spectroscopic setup used at the NLC. See text for detail.

The photoinduced OD changes are calculated as follows:

$$\Delta OD_\lambda = \Delta A_{\text{PumpON}} - \Delta A_{\text{PumpOFF}} = -\log\left(\left(\frac{I_\lambda^{\text{probe}}}{I_\lambda^{\text{ref}}}\right)_{\text{excited}} \middle/ \left(\frac{I_\lambda^{\text{probe}}}{I_\lambda^{\text{ref}}}\right)\right) \qquad (2)$$

where $\left(I_\lambda^{\text{probe}}/I_\lambda^{\text{ref}}\right)_{\text{excited}}$ is a ratio of the pump and reference beam intensities at a specific wavelength λ, which is measured after the sample has been excited; whilst $\left(I_\lambda^{\text{probe}}/I_\lambda^{\text{ref}}\right)$ is the same ratio for an unexcited sample.

The nature of the TA PP data is complicated, and the subsequent interpretation after analysis is even more complex in terms of relating rate constants and results to literature. A number of factors such as the sample preparation process, unstable proteins after isolation, pigment ratios, temperature fluctuations, data measuring process, signal-to-noise ratios, sample refreshing rate, etc., all affect the quality of the data. By increasing the number of averages and reducing the focal beam spot sizes, and working in a dark, enclosed environment, the signal-to-noise ratio increased dramatically.

Time-resolved spectra were analyzed by fitting a model to estimate the rate constants of the various processes using kinetic parameters. We used the Glotaran [9] (Global and Target Analysis) freeware. Information of the ET mechanisms that occur in the LHCII trimer can be obtained from Global analysis in the form of rate constants for the various processes. The ET dynamics, which is typically seen from PP spectroscopy is termed Evolution Associated Difference Spectra (EADS), and decays sequentially with each species (τ) decaying into the subsequent one. For a three-compartmental model we therefore consider the scheme $\tau_1 \rightarrow \tau_2 \rightarrow \tau_3$.
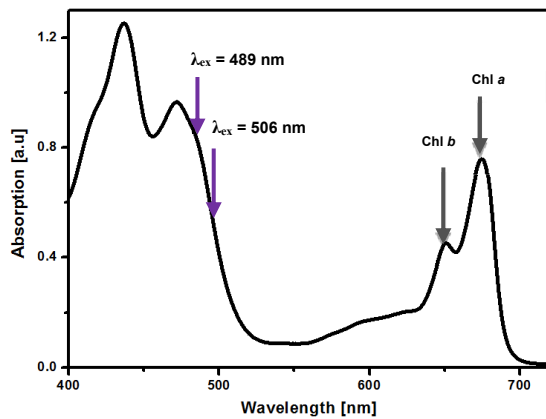
3. Results and Discussion

Figure 3: Measured absorption spectrum of LHCII. Chosen pump excitation wavelengths indicated with arrows – 489 nm and 506 nm. Q_y peak of Chl *a* measured as 0.725/mm. It is important to note that the excitation wavelength of 489 nm is relatively close to the peak of the Chl *b* Soret band, whereas 506 nm more specifically excites the Cars.

Two datasets were acquired from the TA PP measurements on LHCII, pumped at an excitation wavelength (λ_{ex}) of 489 nm and 506 nm, each with an intensity of 500 nJ/pulse. In both cases, a maximum of three kinetic parameters were fitted to the data, until the sequential model converged and a good dispersion fit (3rd order polynomial) was found for each dataset. According to the nature of the individual sample sets, various decay lifetimes were extracted from the data, ranging from a few 100 fs to a few ns – where the latter corresponds to typical fluorescence lifetimes.

The raw TA map upon excitation of LHCII at 506 nm is shown in figure 4(a), while figure 4(b) shows the line spectra at various time delays for the same dataset. The main features are the negative ground state bleach (GSB) around λ_{ex} of 506 nm, excited state absorption (ESA) (central λ = 530 nm), and GSB of Chl *b* (at 650 nm) and Chl *a* (at 673 nm).
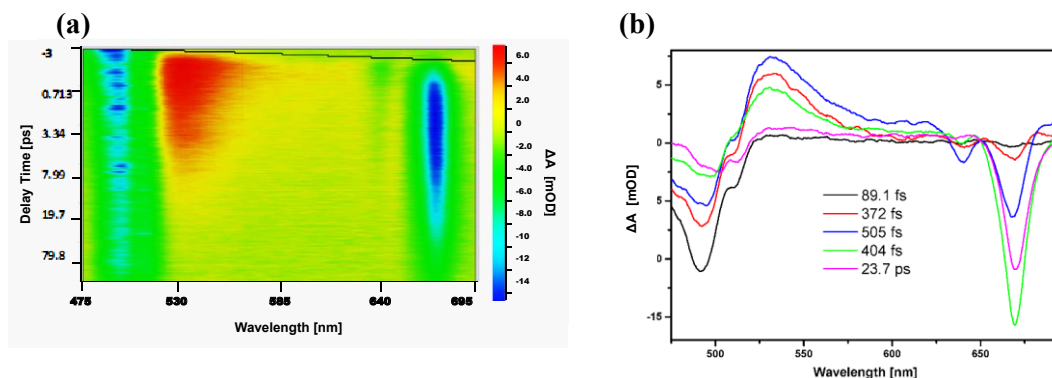

Figure 4: (a) Raw TA data of LHCII pumped at 506 nm with a pulse energy of 500 nJ. The dispersion fit is indicated by the black line. The negative blue/green sections indicate GSB, and positive red the ESA. (b) Spectral evolution (line spectra) of the sample at various delay times.

General trends are seen in the EADS of figure 5, demonstrating the excited ET at specific timescales. The three typical species lifetimes are: $\tau_1 \sim$ 500 fs – 1.5 ps (black line), corresponding to a maximum

pump GSB and decay of the populated Car S_2-state to the other states (see figure 1) as well as maximum ESA. The second species (red) has a lifetime of τ_2 ~10 ps, which corresponds to the fastest decay of the positive ESA band, denoting primarily ET from Car S_1 and Chl *b* to Chl *a* (GSB of the Q_y bands). The third lifetime (blue) has a characteristic lifetime of τ_3 ~600-700 ps and corresponds to relaxation of the Q_y-state of Chl *a*. Since the LHCII is isolated, it is no longer attached to a RC. Hence a surplus of energy remains at Chl *a*, which then results in values that are on the ns timescales and are typical of Chl *a* fluorescence.
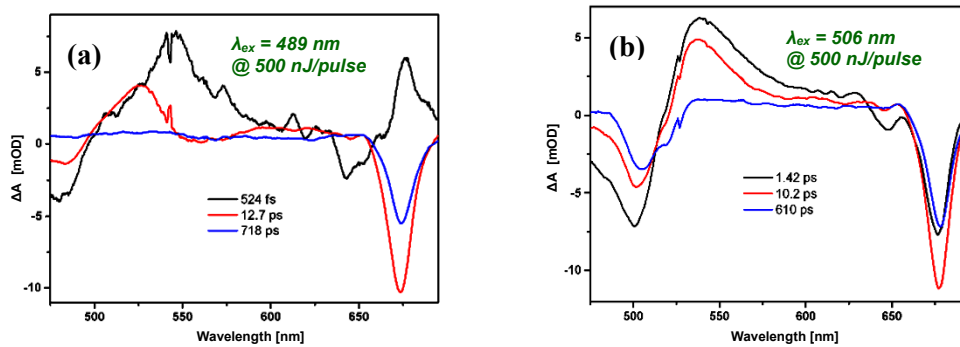

Figure 5: The Evolution Associated Difference Spectra (EADS) of the two LHCII samples investigated under different excitation wavelengths, (a) 489 nm and (b) 506 nm, each with a pulse energy of 500 nJ.

The Chl *b* bleach is stronger in figure 5(a) than in figure 5(b), which can be explained by the excitation in the blue region (489 nm) inferring a higher probability of exciting Chl *b* in the Soret region, as opposed to exciting only the Car region (506 nm). Thus, within the first few ps (τ_2), maximum ET occurs from the initially excited Chl *b* towards Chl *a*, as well as maximum ESA. The first lifetime of figure 5(a) has the structure of a coherent artefact, which arises around time zero as the supercontinuum probe traverses the sample [13]. Upon close inspection, there is a slight wavelength shift of ~5 nm towards the red for λ_{ex} 506 nm of all the bands, which corresponds to equilibrium of the energy before ET of de-excitation. The order of magnitude of the three EADS rate constants correspond to those found earlier in a similar study by Gradinaru, et al. in 2000 [8].
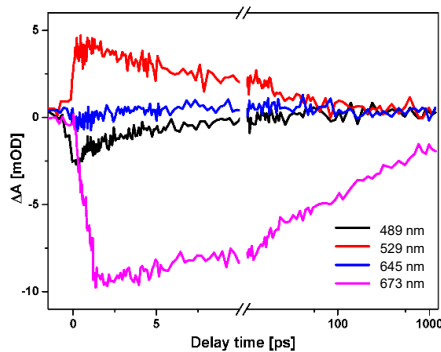

Figure 6: Difference intensity trace, after pumping with 500 nJ/pulse for λ_{ex} of 489 nm. At four characteristic wavelengths we see the following: 489 nm (decay of initially populated Car S_2 state), 529 nm (ESA, and population of Car S_1), 645 nm (Chl *b* peak), and 673 nm (Chl *a* peak).

Figure 6 shows that the decay of each species began around the same time. At first glance, it is apparent that the decay profiles of the λ_{ex} at 489 nm with 500 nJ/pulse excitation are noisy. The strong Chl *a* bleach at 673 nm has the longest rise time, suggesting that this bleach was the dominant processes.

The excitation fluence (number of photons per unit area per pulse) [14] was calculated using a beam diameter of 800 μm for λ_{ex} 489 nm and 506 nm, and pump power of 500 μW. On average, the fluence was measured to be ~10^{17} photons per cm^2 per pulse. According to literature, at this order of magnitude we expect an increase in the singlet-singlet annihilation probabilities [15]. The difference is by and large attributed to the large beam diameter used, and one of the major future prospects is to reduce the focal spot sizes of both the pump and probe beams in the PP system. Hence, a high excitation fluence implies stronger change in absorbance signals, and a greater chance for singlet-singlet annihilation to occur.

4. Conclusion

This paper has highlighted some of the main spectral (at the pigment peaks) and kinetic (species lifetimes) results obtained for the various ET mechanisms amongst the Cars and Chls in the LHCII complex of spinach leaves. The wavelength dependent study, using a pulse energy of 500 nJ for the 489 nm and the 506 nm pump excitations exhibited a clear difference in the sample absorption and ET dynamics, as well as signal strengths (OD). The EADS showed that there is a difference in the ET dynamics between the Car region, and Chl *a* and *b* regions. Using different excitation wavelengths affect the lifetimes of processes, as well as the specific pigments that are targeted in this case. Global analysis gives the overall decay of a system as a whole (mixture of pure molecular states), from which specific elucidation of individual and intermediate states can be performed on the data as target analysis. High excitation fluence values infers a greater chance for singlet-singlet annihilation to occur, resulting in a larger number of molecules relaxing back to the GS. Nonetheless, the kinetic values obtained from this experiment for the various ET mechanisms amongst the Cars and Chls of the LHCII, are a good indication that the setup can be used for more sophisticated data acquisition experiments. In conclusion, the technique of ultrafast pump-probe spectroscopy was successfully applied to the LHCII of spinach leaves, preparing a local South African system to contend on an international platform.

References

[1] Liu Z, Yan H, Wang K, Kuang T, Zhang J, Gui L, An X, Chang W 2004 *Nature* **428** 287

[2] Gradinaru C C, Kennis J T M, Papagiannakis E, van Stokkum I H M, Cogdell R J, Fleming G R, Nierderman R A, van Grondelle R 2001 *PNAS* **98** 2364–69

[3] van Amerongen H, Croce R 2013 *Photosyn. Research* **116** 251-63

[4] Xu P, Tian L, Kloz M, Croce R 2015 *Nature: Scientific Reports* **5** 1-10

[5] Demmig-Adams B, Adams W W 2002 *Science* **298** 2149

[6] Ruban A V, Berera R, Ilioaia C, van Stokkum I H M, Kennis J T M, Pascal A A, van Amerongen H, Robert B, Horton P, van Grondelle R 2007 *Nature* **450** 575-9

[7] Ostroumov E E, Mulvaney R M, Cogdell R J, Scholes G D 2013 *Science* **340** 52-6

[8] Gradinaru C C, van Stokkum I H M, Pascal A A, van Grondelle R, van Amerongen H 2000 *J. Phy. Chem. B* **104** 9330-42

[9] Snellenburg J J, Laptenok S P, Seger R, Mullen K M, van Stokkum I H M 2012 *J. Stat. Soft.* **49** 1-22

[10] Van Roon H, van Breemen J F L, der Weerd F L, Dekker J P, Boekema E J 2000 *Photosyn. Research* **64** 155–66

[11] von Leeuwen P J, Nieveen M C, van der Meent E J, Dekker J P, van Gorkom H J 1991 *Photosyn. Research* **28** 149-53

[12] Blankenship R E, Molecular Mechanisms of Photosynthesis, Blackwell Science Ltd, Oxford 2002

[13] Lebedev M V, Misochko O V, Dekorsy T, Georgiev N 2005 *J. Exp. & Theo. Phys.* **100** 272-82

[14] Zaushitsyn Y, Jespersen K G, Valkunas L, Sundström V, Yartsev A 2007 *Phys. Review* B **75** 1952011-17

[15] Schödel R, Hillmann F, Schrötter T, Voigt J, Irrgang K D, Renger G 1996 *Biophys. J* **71** 3370-80